HAGFISH
BIOLOGY

Edited by

Susan L. Edwards
Gregory G. Goss

CRC Press
Taylor & Francis Group

HAGFISH

BIOLOGY

CRC

MARINE BIOLOGY

SERIES

The late Peter L. Lutz, Founding Editor
David H. Evans and Stephen Bortone, Series Editors

PUBLISHED TITLES

Biology of Marine Birds
E.A. Schreiber and Joanna Burger

Biology of the Spotted Seatrout
Stephen A. Bortone

Early Stages of Atlantic Fishes: An Identification Guide for the Western Central North Atlantic
William J. Richards

Biology of the Southern Ocean, Second Edition
George A. Knox

Biology of the Three-Spined Stickleback
Sara Östlund-Nilsson, Ian Mayer, and Felicity Anne Huntingford

Biology and Management of the World Tarpon and Bonefish Fisheries
Jerald S. Ault

Methods in Reproductive Aquaculture: Marine and Freshwater Species
Elsa Cabrita, Vanesa Robles, and Paz Herráez

Sharks and Their Relatives II: Biodiversity, Adaptive Physiology, and Conservation
Jeffrey C. Carrier, John A. Musick, and Michael R. Heithaus

Artificial Reefs in Fisheries Management
Stephen A. Bortone, Frederico Pereira Brandini, Gianna Fabi, and Shinya Otake

Biology of Sharks and Their Relatives, Second Edition
Jeffrey C. Carrier, John A. Musick, and Michael R. Heithaus

The Biology of Sea Turtles, Volume III
Jeanette Wyneken, Kenneth J. Lohmann, and John A. Musick

The Physiology of Fishes, Fourth Edition
David H. Evans, James B. Claiborne, and Suzanne Currie

Interrelationships Between Coral Reefs and Fisheries
Stephen A. Bortone

Impacts of Oil Spill Disasters on Marine Habitats and Fisheries in North America
J. Brian Alford, PhD, Mark S. Peterson, and Christopher C. Green

Hagfish Biology
Susan L. Edwards and Gregory G. Goss

HAGFISH
BIOLOGY

Edited by
Susan L. Edwards
Appalachian State University, Boone, North Carolina, USA
Gregory G. Goss
University of Alberta, Edmonton, Alberta, Canada

CRC Press
Taylor & Francis Group
Boca Raton London New York

CRC Press is an imprint of the
Taylor & Francis Group, an **informa** business

CRC Press
Taylor & Francis Group
6000 Broken Sound Parkway NW, Suite 300
Boca Raton, FL 33487-2742

Version Date: 20150708

International Standard Book Number-13: 978-1-4822-3346-9 (eBook - PDF)

Contents

Preface

The hagfishes are a cosmopolitan group of craniate chordates, inhabiting almost all the oceans of the world, other than Antarctica. Hagfishes as craniates do not have vertebrae but do possess cranial bones and are considered to be the most ancient of the jawless fishes, having diverged from the main vertebrate lineage more than 500 million years ago. That hagfishes are physiologically unique in that they are the only living craniates to maintain their plasma NaCl concentration almost the same as that of seawater is a feature that has been known for almost 100 years. However, new high-throughput sequencing technologies allowing for improved genetic information, advanced microscopy techniques, the recent description of hagfish embryology, and the development of techniques to understand ancient evolutionary relationships have together led to a resurgence in interest in the hagfish as a key species to understand the evolution of the vertebrates.

These advances have resulted in new perspectives in hagfish research and this has led to the development of this new compendium of information on the hagfishes. An important part of putting this publication together was the gathering of hagfish biologists from all over the world in a symposium at the International Congress on the Biology of Fishes held in Edinburgh, Scotland, August 2014. This book aims to build on our previous knowledge and further expand the scientific interest for this fascinating yet understudied key evolutionary species. We hope that this book leads to a larger conversation and provides the impetus for new research avenues to develop.

Editors

Susan L. Edwards, PhD, is a professor of biology and chairperson at Appalachian State University in Boone, NC. She received her BSc in biology from Deakin University in 1994, her MSc in neuroscience from the University of Melbourne in 1997, and earned a PhD in comparative physiology from Deakin University in 2000. Her postdoctoral studies were conducted with Dr. James B. Claiborne at Georgia Southern University. In 2002, she took her first academic position in Queensland, Australia at James Cook University. However, in 2006, after many years of commuting from Australia to the United States for research, she decided to relocate to the United States to be closer to her model organisms.

Dr. Edwards' research program is focused on the identification and localization of ion transport mechanisms associated with osmotic balance, acid/base homeostasis, and more recently nitrogenous waste excretion in fishes. She is an active member of the American Fisheries Society and is the president-elect of the physiology section. She is also a member of the Canadian Society of Zoology, Society for Experimental Biology, Australian and New Zealand Society of Comparative Physiology and Biochemistry, and is a life member of the Mount Desert Island Biological Laboratory. She serves on the editorial board of *Comparative Biochemistry and Physiology* and has served on a number of panels for the National Science Foundation.

Gregory G. Goss, PhD, is a professor in the Department of Biological Sciences at the University of Alberta and is cross-appointed to the School of Public Health and a Fellow of the National Institute of Nanotechnology. Dr. Goss was appointed assistant professor in July 1997 and held ranks of associate and full professor in July of 2002 and 2005, respectively. Prior to his faculty position, Dr. Goss held two postdoctoral appointments at Hospital for Sick Children, Toronto, Ontario, and Beth Israel Hospital, Harvard Medical School, Boston, MA. He completed his BSc (1986) and MSc (1988) at McMaster University with Professor Chris M. Wood and obtained a PhD (1993) at the University of Ottawa under the tutelage of Professor Steve Perry. He is the past winner of the Petro-Canada Young

Innovator Award, the Canadian Society of Zoologists Early Investigator Award, the American Physiological Society Young Investigator Award, the McCalla award for teaching and research, and was awarded a Killam Annual Professorship in 2009–2010.

Dr. Goss' research is focused on the twin areas of toxicology and comparative physiology in a variety of fish species. In addition to his research at the University of Alberta, he regularly conducts his research program at Bamfield Marine Sciences Centre (BMSC), where he leads a productive program aimed at understanding the physiology of ion, acid–base, and solute transport regulation in trout, dogfish, and hagfish. It is at BMSC where Dr. Goss became acutely interested in hagfish physiology and thus formed the impetus for this book. Dr. Goss has served as president of the Canadian Society of Zoologists and serves on the council for numerous national and international societies. He is an associate editor of the *Canadian Journal of Zoology* and on the editorial boards for *Nanotoxicology and Environmental Science: Nano.*

Contributors

William C. Aird
Department of Medicine
Beth Israel Deaconess Medical Center
Harvard Medical School
Boston, Massachusetts

Carol Bucking
Department of Biology
York University
Toronto, Ontario, Canada

Nic R. Bury
Diabetes and Nutritional Sciences Division
King's College London
London, United Kingdom

Alexander M. Clifford
Department of Biological Sciences
University of Alberta
Edmonton, Alberta, Canada

Michael I. Coates
Department of Organismal Biology and Anatomy
University of Chicago
Chicago, Illinois

Shaun P. Collin
School of Animal Biology and the Oceans Institute
The University of Western Australia
Crawley, Western Australia, Australia

Max D. Cooper
Department of Pathology and Laboratory Medicine
Emory University School of Medicine
Atlanta, Georgia

Sabyasachi Das
Department of Pathology and Laboratory Medicine
Emory University School of Medicine
Atlanta, Georgia

William Davison
School of Biological Sciences
University of Canterbury
Christchurch, New Zealand

Ann M. Dvorak
Department of Pathology
Beth Israel Deaconess Medical Center
Harvard Medical School
Boston, Massachusetts

Susan L. Edwards
Department of Biology
Appalachian State University
Boone, North Carolina

Douglas S. Fudge
Department of Integrative Biology
University of Guelph
Guelph, Ontario, Canada

Chris N. Glover
School of Biological Sciences
University of Canterbury
Christchurch, New Zealand

Gregory G. Goss
Department of Biological Sciences
University of Alberta
Edmonton, Alberta, Canada

Scott M. Grant
Centre for Sustainable Aquatic Resources
Marine Institute of Memorial University of Newfoundland
St. John's, Newfoundland and Labrador, Canada

Julia E. Herr
Department of Integrative Biology
University of Guelph
Guelph, Ontario, Canada

Brantley R. Herrin
Department of Pathology and Laboratory Medicine
Emory University School of Medicine
Atlanta, Georgia

Masayuki Hirano
Department of Pathology and Laboratory Medicine
Emory University School of Medicine
Atlanta, Georgia

Philippe Janvier
Muséum National d'Histoire Naturelle
UMR7207 (CNRS, Sorbonne Universités, UPMC, MNHN)
Paris, France

Trevor D. Lamb
Department of Neuroscience and ARC Centre of Excellence in Vision Science
Australian National University
Canberra, Australia

Jianxu Li
Department of Pathology and Laboratory Medicine
Emory University School of Medicine
Atlanta, Georgia

Tetsuto Miyashita
Department of Biological Sciences
University of Alberta
Edmonton, Alberta, Canada

Masumi Nozaki
Sado Marine Biological Station
Niigata University
Niigata, Japan

Jinae N. Roa
Marine Biology Research Division
University of California San Diego
La Jolla, California

Robert S. Sansom
Faculty of Life Sciences
University of Manchester
Manchester, United Kingdom

Stacia A. Sower
Department of Molecular, Cellular and Biomedical Sciences
University of New Hampshire
Durham, New Hampshire

Martin Tresguerres
Marine Biology Research Division
University of California San Diego
La Jolla, California

Alyssa M. Weinrauch
Department of Biological Sciences
University of Alberta
Edmonton, Alberta, Canada

Timothy M. Winegard
Department of Integrative Biology
University of Guelph
Guelph, Ontario, Canada

chapter one

Anatomy of the Pacific hagfish (Eptatretus stoutii)

Alyssa M. Weinrauch, Susan L. Edwards, and Gregory G. Goss

Contents

Introduction

Collectively, hagfishes are among the earliest extant members of the vertebrate lineage. Although there have been multiple reports detailing the histology and gross morphology of various tissues, a comprehensive atlas

of the hagfish that includes gross morphology, histology, and electron microscopy has never been created before. This chapter will provide a source for understanding the fundamental histology of cells and tissues in the Pacific hagfish (*Eptatretus stoutii*). By combining physiological studies with the described anatomy, we will be able to better elucidate the evolution of physiological and morphological traits.

Tissue histology

Integument

Hagfish lack scales and an outer *stratum corneum* (Figure 1.1a). Instead, the outer layer is homologous to the *stratum germinitavium* found in vertebrates. Resting atop a layer of skeletal muscle are the epidermis (E), dermis (D), and hypodermis (Andrew and Hickman, 1974). The epidermal layer is 75–200 μm thick, with variances depending on species, nutritional state, and location along the body (Andrew and Hickman, 1974). It is comprised of four cell types, held together by desmosomes (Spitzer and Koch, 1998): undifferentiated cells (UC), small mucous cells (SMC), large mucous cells (LMC), and epidermal thread cells (ETC) (Figure 1.1b) (Blackstad, 1963; Andres and von Düring, 1993; Spitzer and Koch, 1998). Mucous cells are thought to be homologous to goblet cells and are constitutively expressed in the epidermis, forming near the basement membrane (BM) and migrating to the epidermis to release their contents as they mature (Andrew and Hickman, 1974). Small mucous cells are regular in shape (diameter averaging ~12.4 μm), whereas large mucous cells are ellipsoidal, becoming more elongated as they reach the epidermal surface (diameter averaging ~31.2 μm). The nucleus (N) is large, with cytoplasmic filaments compacted to the basal and lateral sides of differentiated cells and prominent nucleoli (Ni) observed throughout all cell types (Figure 1.1c). The large mucous cells nuclei stain darkly but the diffuse cytoplasmic components stain weakly highlighting contrast, whereas the scanning electron microscopy (SEM) enhances the fusion and release of mucous contents from the clustering mucous cells, as well as the ~0.25–0.55 μm long projections on the surface (microplicae (MP)) (Figures 1.1c–e). The functions of the epidermal thread cells (diameter averaging ~19.8 μm) are undefined to date, however some speculate that the threads and mucous cells act like the slime glands to yield additional slime (Spitzer and Koch, 1998). Staining techniques employed in our study of *E. stoutii* have appeared to unravel the threads, leaving an acidic granular product within the epidermal thread cells (Figure 1.1b1). When different staining protocols are used, the thread-like nature of *Myxine glutinosa* epidermal thread cells can be observed (Figure 1.1b2; kindly provided by Sarah Schorno, Tim Winegard, and Dr. Douglas Fudge).

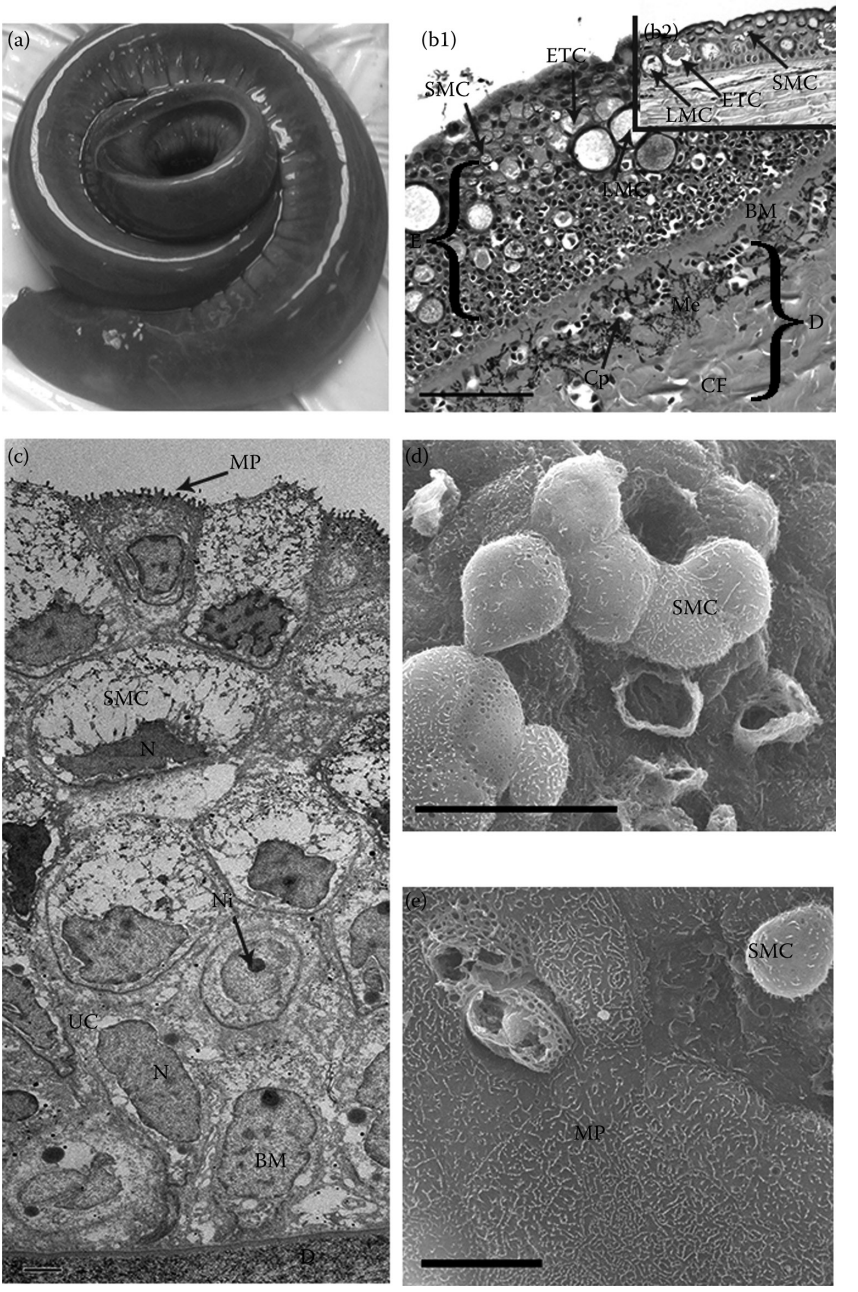

Figure 1.1 **(See color insert.)** (*Continued*)

Specialized cell types include the flask-shaped sensory Schreiner organs and ionocytes, which, although not shown here, are infrequently dispersed throughout the skin (Braun, 1998; Spitzer and Koch, 1998). The precise sensory function of the Schreiner organ is yet to be determined. A unique basement membrane with a basal lamina on both sides separates the dermis from the epidermis, and housed within this layer are hormonally controlled melanocytes (Me) containing brown/black melanin granules (Coonfield, 1940; Andrew and Hickman, 1974). Both the dermo-epidermal and the dermo-hypodermal junctions contain elastic-like fibers that are difficult to stain. The dermis is comprised of 5–10 μm thick collagen fibers (CF), providing the elasticity necessary for undulation during swimming (Andrew and Hickman, 1974; Welsch et al., 1998). Numerous capillaries (Cp) filled with erythrocytes (RBC) occur throughout the dermis, permitting gas exchange and possibly supplying mucous cells with mucous composites (Figure 1.1b) (Potter et al., 1995). Reduced vascularization is observed in *Myxine* sp. when compared with *Eptatrids* sp., likely because of their burrowing behavior. The hypodermis is comprised of loose connective tissues (CT), blood vessels, and glycogen-rich adipose tissue (Blackstad, 1963; Andrew and Hickman, 1974).

Sensory barbels

Hagfish have limited visual capacity, having only eye spots rather than compound eyes (see Chapter 6). Thus, they rely heavily on mechanosensation using their barbels to perceive their surroundings (Greene, 1925),

***Figure 1.1* (*Continued*)** Integument. (a) Gross morphology of *E. stoutii* demonstrating the scale-less nature of hagfish skin. (b) Light micrograph demonstrating the cellular morphology of the dermis and epidermis of hagfish integument. (b1) A 75–200 μm thick epithelium (E) is comprised of four distinct cell types: undifferentiated cells (UC), small mucous cells (SMC), large mucous cells (LMC), and epidermal thread cells (ETC). These rest upon a basement membrane (BM), which sits atop the dermis (D) comprised of collagen fibers (CF) and housing the pigment-containing melanocytes (Me) and numerous capillary (Cp) networks. H&E stain. Scale bar = 100 μm. (b2) Light micrograph of *M. glutinosa* epidermis highlighting the coiled, thread-like nature of the ETCs that were not found to be as distinct in *E. stoutii*. Scale bar = 25 μm. Photograph kindly provided by Sarah Schorno, Tim Winegard, and Dr. Douglas Fudge. (c) Transmission electron micrograph of *E. stoutii* skin highlighting the microplicae (MP) on the epithelial surface along with the prominent nucleoli (Ni) within the basolaterally located nuclei (N) and diffuse surrounding cytoplasm. UCs are strikingly different with a central nucleus and more compact cytoplasm. Scale bar = 2 μm. (d) Scanning electron micrograph of *E. stoutii* epidermis. The clustering of SMCs is apparent alongside cells that have burst to release their contents. Scale bar = 20 μm. (e) Scanning electron micrograph of *E. stoutii* integument demonstrating the ubiquitous distribution of MP around and on the SMCs. Scale bar = 10 μm.

although a role for chemosensation cannot be ruled out. Notably, when the hagfish coils, the head is consistently on the outside of the coil exposing the sensory barbels (SB), of which there are three pairs in *Eptatretus* sp. that surround the nasohypophysial opening (NO) (Figure 1.2a) (Greene, 1925). These barbels oscillate both while swimming and at rest, suggesting a mechanosensory function that is sensitive throughout the barbel (Worthington, 1905; Greene, 1925; Blackstad, 1963; Andrew and Hickman, 1974). Hagfish barbels are similar to catfish tentacles, which contain numerous goblet cells and have been characterized using various stains (Yan, 2009). Catfish tentacles are present only in males as a result of sexual dimorphism, with the mucous cell components thought to provide nourishment for the larvae as the males alone care for the young (Yan, 2009), although no apparent sexual dimorphisms exist in hagfishes. Morphologically, the sensory barbel contains an outer epithelium (E) with distinct basolateral congregation of nuclei within each cell type: as in the skin, the epidermis is comprised of small mucous cells and undifferentiated cells resting on a basement membrane, whereas large mucous cells and epidermal thread cells are not observed. Also consistent with other integument is the presence of microplicae on the outer surface. The underlying dermis (D) is consistent with the aforementioned description, complete with abundant capillary (Cp) networks and melanocytes, however the underlying layer contains muscular tissue (Ms) and connective tissue, along with a small pocket of cartilage (Crt), permitting rigidity, control, and oscillation of the tentacles (Figures 1.2b–e). This could allow the tentacles to remain sentient when facing a strong force, for example, during active predation (Zintzen et al., 2011). Sensory Schreiner organs are evident and abundant, as long, conical cells located in sensory buds (SBd) deep in the epidermis and extending to the surface (Blackstad, 1963; Braun, 1998), with flagellated structures observable in the SEM images (Figures 1.2f1 and f2) that seem to be lost during other fixation procedures (e.g., TEM, light microscopy).

Dental plate

Hagfish are demersal opportunistic scavengers known to feed on a wide variety of decaying animals ranging from polychetes and mollusks to mammals (Martini, 1998; Clark and Summers, 2007, 2012; Glover et al., 2011). Recent video evidence from Zintzen et al. (2011) also demonstrates a predatory behavior in some species (*Neomyxine*), where possible suffocation by slime exudate occurs within burrows. Although this behavior could be universal across the *Myxine*, it is currently unknown how many hagfish species utilize active predation and if used, how often in comparison to decaying ocean fall (Zintzen et al., 2011). Morphological similarities between juvenile and adult hagfish

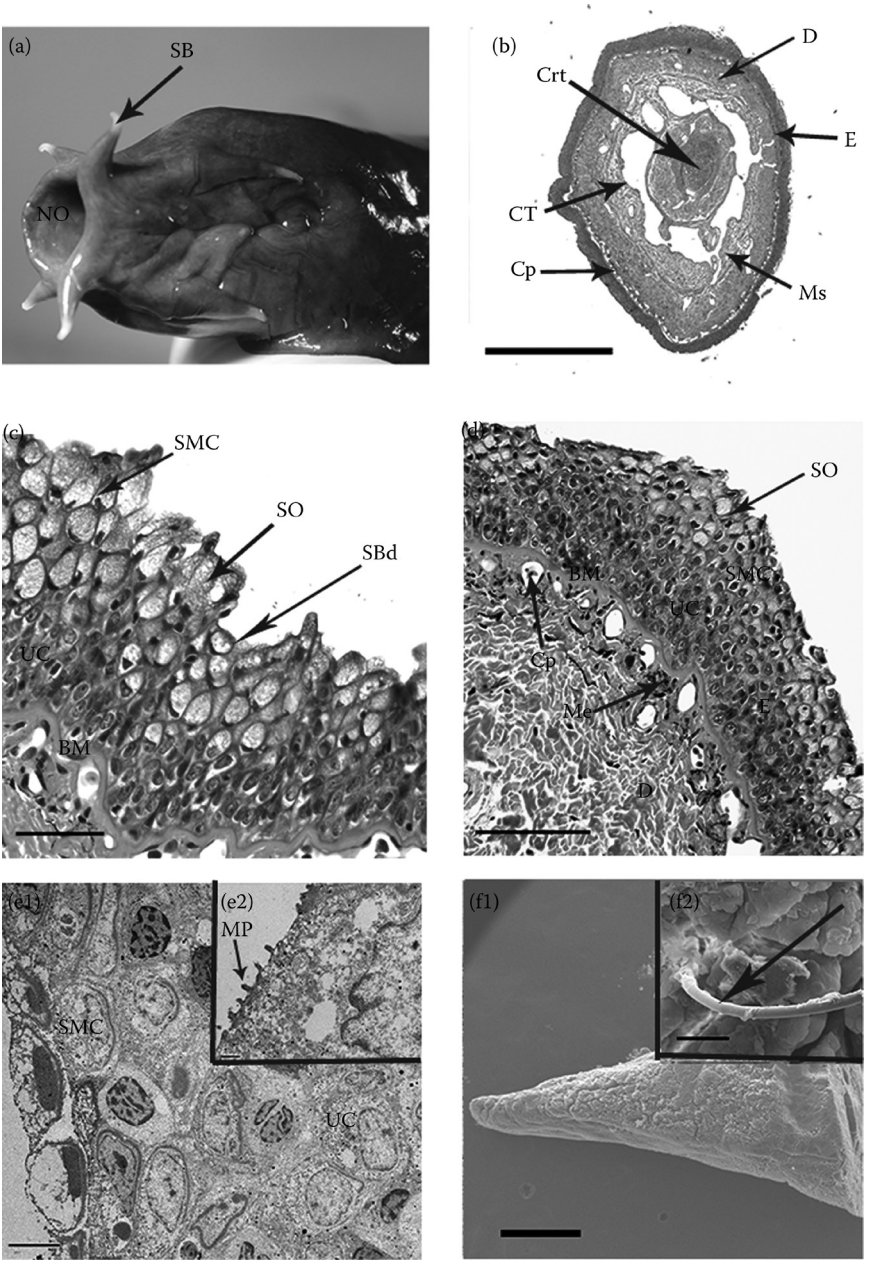

Figure 1.2 **(See color insert.)** (*Continued*)

teeth are suggestive of similar diets throughout the hagfish life history, as well as between species (*Myxine* and *Eptatrids*) (Clark and Summers, 2012). Detection of food appears to occur via smell and touch with the sensory barbels (Clark and Summers, 2007).

Continual protraction and retraction of a heart-shaped dental plate, housing two rows of conical teeth (T), tear tissues from carrion and permits entry into the body cavity (Figure 1.3a) (Dawson, 1963; Krejsa et al., 1990; Clark and Summers, 2007, 2012; Chiu et al., 2011). Recent studies determined that hagfish acquire nutrients/ions via extraintestinal means such as the skin (Glover et al., 2011; Schultz et al., 2014), and perhaps entry into carrion enhances uptake.

Plate movement occurs as a result of protractor and retractor muscles (see pharyngeal muscle) with produced force being equivalent to that of some gnathostomes despite the lack of bone used for muscle attachment (Dawson, 1963; Krejsa et al., 1990; Clark and Summers, 2007, 2012; Chiu et al., 2011). The force of penetration, as well as tooth stress, alters the tearing ability, whereas the ability to grasp prey is proportional to tooth number and surface area (Clark and Summers, 2012).

The dental plate houses a single palatine tooth responsible for continued hold on prey, as well as two rows of bilaterally symmetrical lingual teeth (7–9 per row) for rasping (Dawson, 1963; Slavkin et al., 1983; Rice et al., 1994; Clark and Summers, 2007, 2012). Hagfish ranging 98–202 mm in length have palatal teeth 0.5–1.5 mm in length, whereas the outer and inner rows of lingual teeth are 1.6–3.8 and 1.9–4.5 mm in length, respectively (Krejsa et al., 1990). The lingual teeth change orientation and fold into one another during plate retraction, rasping at decaying flesh (Clark and Summers, 2012).

***Figure 1.2* (*Continued*)** Sensory barbels (SB). (a) A gross morphological representation of the three pairs of SBs surrounding the nasohypophysial opening (NO) in Pacific hagfish. (b) Transverse section of SB demonstrating the layers within. The outer epithelial layer (E) rests atop a dermis (D) housing the capillaries (Cp). Beneath this layer are layers of connective tissue (CT) and muscle (Ms), surrounding a small central pocket of cartilage (Crt). H&E Stain. Scale bar = 1 mm. (c) Sagittal section of hagfish SBs. Resting atop a basement membrane (BM) are undifferentiated cells (UC), which migrate to the surface and differentiate into small mucous cells (SMC). Also abundant are sensory Schreiner organs (SO), which form sensory buds (SBd) thought to hold flagella. H&E stain. Scale bar = 50 µm. (d) Sagittal section of hagfish barbel demonstrating the cellular composition of the epidermis (e) containing UCs, SMCs, and SOs. Beneath the BM is the dermis (d) housing the capillaries (Cp) and melanocytes (Me). H&E stain. Scale bar = 100 µm. (e) Transmission electron microscopy detailing the differentiated SMCs atop the UC (e1) and microplicae (MP) (e2). Scale bar = 5 µm. (f) Scanning electron micrograph of the SB highlighting the rough surface (f1). Scale bar = 500 µm. Long flagellated structures (arrow) were observed using SEM and are possible components of the SOs (f2). Scale bar = 50 µm.

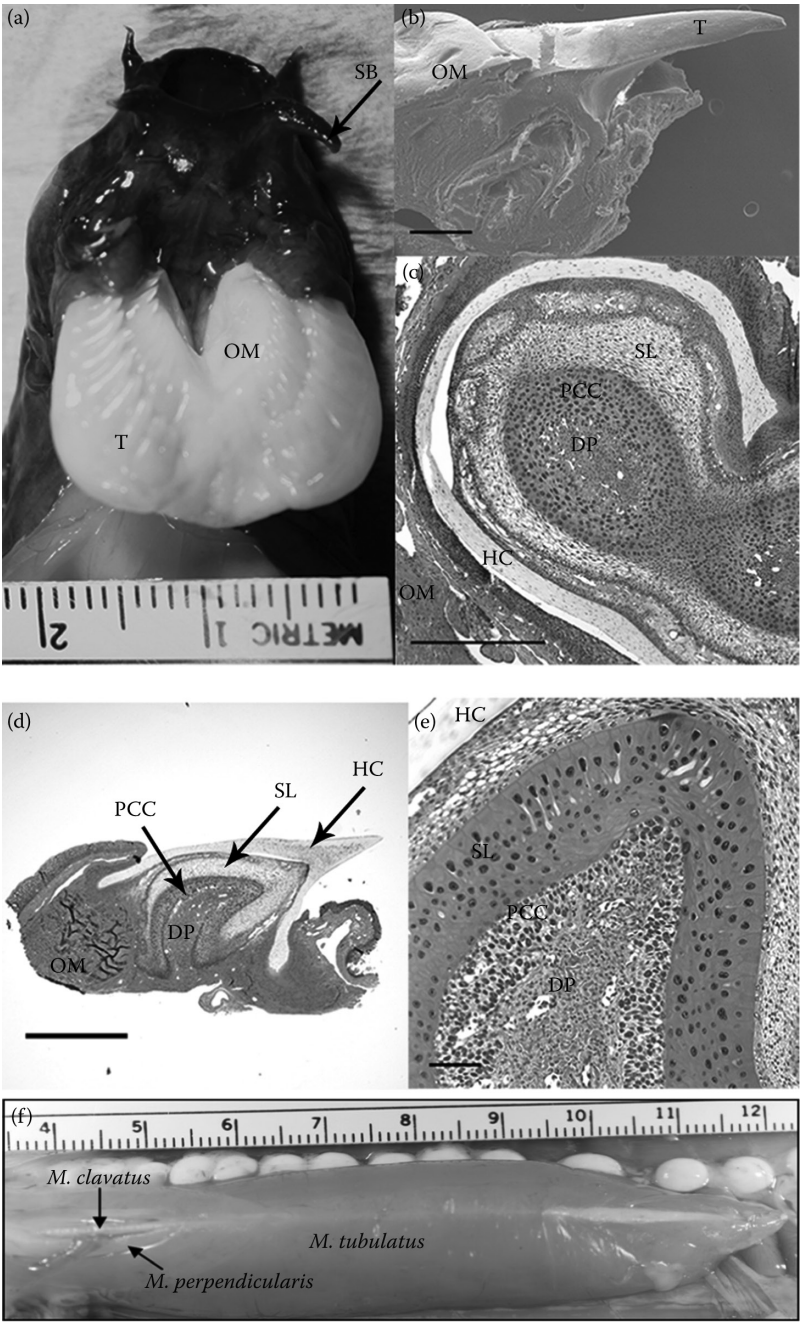

Figure 1.3 **(See color insert.)** (*Continued*)

The tooth is comprised of multiple "cone" layers, making it conducive to postprandial tooth replacement (Dawson, 1963; Krejsa et al., 1990; Clark and Summers, 2007, 2012). The tooth replacement process is similar to squamate integument shedding and also follows typical vertebrate tooth formation until crown formation where the dentin–protein complex forms. This is because cyclostomes lack calcified structures and thus enamel and dentin are not present; however, an enamel-like protein of unknown function has been discovered and is suggestive of the conservation of enamel protein structure throughout vertebrate evolution (Slavkin et al., 1983; Krejsa et al., 1990; Clark and Summers, 2012). The layers composing the tooth include the central dental papilla (DP), pokal cell cone (PCC), stellate layer (SL), and outer horn cap (HC), all of which rest in the oral mucosa (OM) (Figure 1.3a–e) (Dawson, 1963; Krejsa et al., 1990; Clark and Summers, 2007, 2012).

The dental papilla is the site of new tooth formation (Krejsa et al., 1990), which eventually gives rise to the pokal cell cone, or functional tooth. This area is rich in lipids and phospholipids, providing the structural support for the tooth. Moving outward, the stellate layer is incredibly vacuolated and these cells produce the keratinous outer horn cap and separate the outer shedding tooth from the underlying replacement (Dawson, 1963). These cells are also found in lamprey and are thought to be synonymous to the stellate reticulum of gnathostomes (Krejsa et al., 1990). Some adults have multiple stellate layers and pokal cell cones to increase the rapidity of tooth replacement (Krejsa et al., 1990). The keratinous horn cap provides the strength and shape of the tooth, with elongated cells at the apex representing pokal cell remnants (Appy and Anderson, 1981; Krejsa et al., 1990; Clark and Summers, 2012).

***Figure 1.3* (*Continued*)** Dental plate. (a) Gross morphology of the hagfish dental plate. The sensory barbels (SB) surrounding the nasopharyngeal opening and mouth presumably detect food sources. The hagfish then repeatedly everts and retracts the dental plate where two rows of teeth (T) sit in an oral mucosa (OM). (b) Scanning electron micrograph of a hagfish tooth (T) still intact with the OM. Scale bar = 500 µm. (c) Transverse section of a hagfish tooth demonstrating the "cone within a cone" makeup of the tooth within the OM. The central dental papilla (DP) initiates tooth growth into the pokal cell cone (PCC) otherwise known as the functional tooth. Residing atop this layer is the stellate layer (SL), which produces the outer keratinous horn cap (HC). H&E stain. Scale bar = 500 µm. (d) Sagittal representation of the hagfish tooth resting in OM. The central DP forms the functional tooth known as the PCC. Atop this rests the SL, which produces the outer keratinous horn cap (HC). H&E stain. Scale bar = 1 mm. (e) Higher magnification of the pokal cell layers, as above. H&E stain. Scale bar = 100 µm. (f) Gross anatomical portrait of the pharyngeal muscles. It is comprised of two muscles in concentric rings: the outer *M. tubulatus* and the inner *M. clavatus*. Also evident is the *M. perpendicularis* running between the paired *M. clavatus* muscle.

Dental muscle (pharyngeal muscle)

The dental plate is maneuvered using a set of protractor and retractor muscles. Specifically, the retractor muscles include the *M. tubulatus*, *M. elevatus*, and *M. perpendicularis*, all enclosed within a sheath of connective tissue (Figure 1.3f). *M. tubulatus* is a paired muscle that forms an outer ring of muscle surrounding the inner *M. clavatus*, which attaches to the posterior edge of the dental plate (Figure 1.4a) (Dawson, 1963; Baldwin et al., 1991). The muscle attaches to the cartilaginous cranium (Clark and Summers, 2012), and transference of force to the dental plate occurs via the clavatus tendon, which has properties similar to those of some gnathostomes (Clark and Summers, 2007). It is comprised of thin white muscle only, as opposed to the white, red, and intermediate fibers that make up the somatic muscle (Clark and Summers, 2007; Chiu et al., 2011). The white muscle can exert rapid and powerful force in anaerobic conditions, whereas the red muscle contracts for extended periods of time with little force (Dawson, 1963; Baldwin et al., 1991). Furthermore, the somatic and pharyngeal muscles differ in enzymatic activity, with the dental muscle having a higher overall activity, apart from those enzymes involved in aerobic catabolism of carbohydrates and lipids (Chiu et al., 2011). This striated muscle (StM) contains few nuclei, however glycogen granules are abundant (Figure 1.4b).

Somatic muscle

Muscles are necessary for movement and therefore feeding and ventilation, however they also act in storage and as energy reserves. The muscle tissue of hagfish is iso-osmotic to seawater, holding concentrations of inorganic ions below that of the plasma (Currie and Edwards, 2010). Hagfish have three distinct muscular groups: *M. parietalis*, *M. obliquus*, and *M. rectus*, with *M. parietalis* constituting the majority of the body, running from nasal to caudal end and extending laterally from the midline to the slime glands (Jansen and Andersen, 1963; Korneliussen and Nicolaysen, 1973). It is comprised of W-shaped metameric segments, as opposed to the common V-shape of other teleosts. Less-developed metameric segments account for the reduced swimming speeds demonstrated by the hagfish (Jansen and Andersen, 1963; Andrew and Hickman, 1974).

Striated muscle fibers (StM), themselves made up of myofibrils, contain numerous nuclei (Figure 1.4e) (Jansen and Andersen, 1963; Hardisty, 1979) and are found in the ~3 mm long myotomes. The myotomes (Mto) are segmented by myosepta (Msp) (tissues containing vascular and nervous elements) (Figures 1.4c and g) (Jansen and Andersen, 1963; Mellgren and Mathisen, 1966) into compartments, with lateral and ventral linings of red fibers and white fibers in the remaining space (Mellgren and Mathisen, 1966). The makeup of the muscle is consistent with that

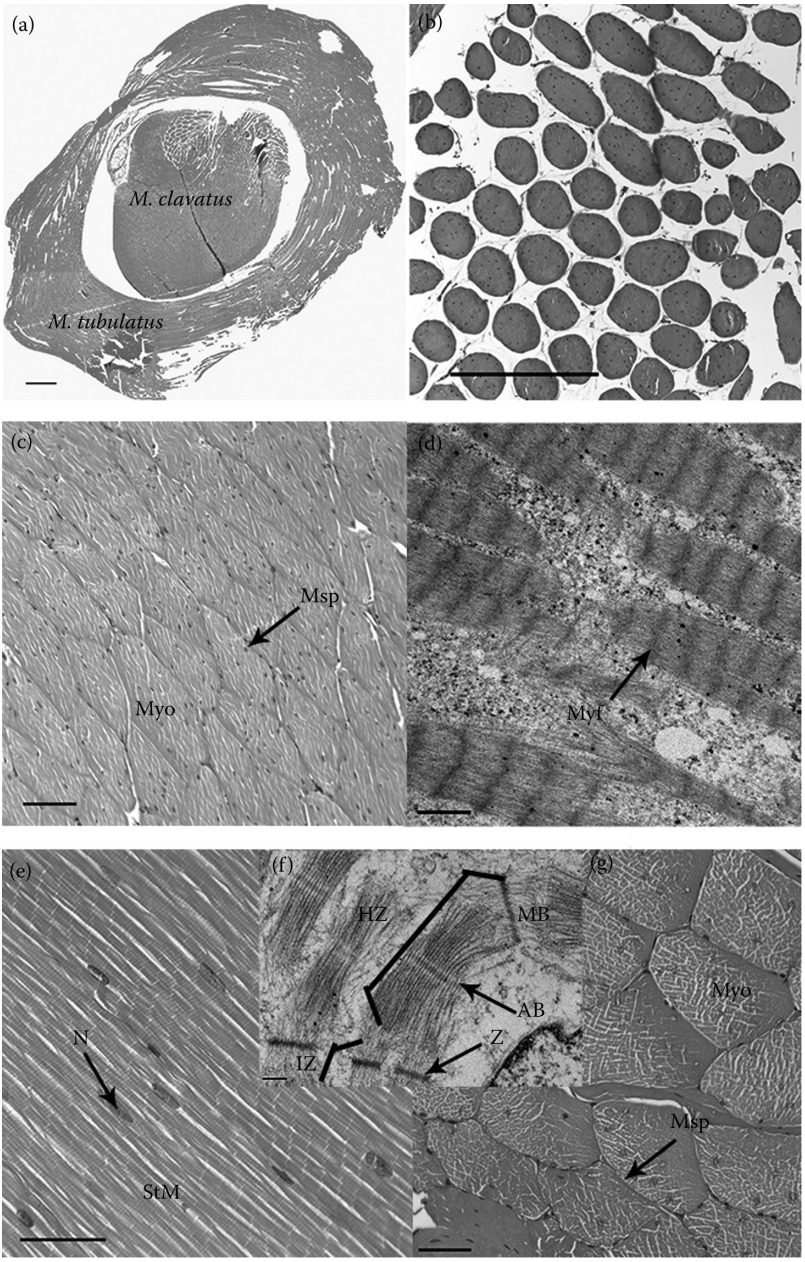

Figure 1.4 **(See color insert.)** (*Continued*)

typically observed in vertebrates being comprised of Z lines, I bands, A bands, and M and H zones (Figures 1.4d and f). These myotomes contain both small, aerobic slow red fibers and large, anaerobic fast white fibers, with 14% of the red fiber surface covered in capillaries and only 0.4% of the white fibers (Jansen and Andersen, 1963; Korneliussen and Nicolaysen, 1973; Baldwin et al., 1991). Within the red fibers are extensive lipid and glycogen deposits (Baldwin et al., 1991), demonstrating the energy reserve capacity of the tissue as opposed to the white tissue, which lack these structures (Mellgren and Mathisen, 1966). Not pictured are *M. obliquus* which forms a thin sheet over *M. parietalis* in the cloacal region, as well as *M. rectus*; a narrow band of muscle running between the slime glands and ventral midline (Jansen and Andersen, 1963).

Intestine

The cyclostome intestine is thought to have derived from the microphagous feeding of ancestral craniates (Appy and Anderson, 1981). As in some fish, hagfish do not have a defined stomach or a differentiated small and large intestine (Andrew and Hickman, 1974; Menke et al., 2011), thus digestion occurs directly in the straight intestinal tube via lipases (Adam, 1963). The intestine is anchored to the body wall, with mesentery containing nerves, blood, and lymph vessels, which is removed in the photograph (Figure 1.5a) (Adam, 1963). Hemocytopoietic tissue and adipose submucosa constitute further portions of the alimentary canal, along with other derivatives such as the liver, biliary system, and pancreas (Jordan and Speidel, 1930; Papermaster et al., 1962; Clark and Summers, 2007). Differences in external gross morphology can be observed between the pharyngocutaneous duct (foregut) and the hindgut, which are separated in the region of the portal

***Figure 1.4* (*Continued*)** Musculature. (a) Light micrograph showing a sagittal section of the pharyngeal muscle that controls the dental plate. The muscles are paired and align in concentric circles with the *M. tubulatus* surrounding the *M. clavatus*. H&E stain. Scale bar = 1 mm. (b) Transverse section of the pharyngeal muscle demonstrating the longitudinal band arrangement. H&E stain. Scale bar = 500 µm. (c) Transverse section of the parietal muscle. Individual multinucleated myomeres (Myo) are tightly joined by myosepta (Msp). H&E stain. Scale bar = 100 µm. (d) Transmission electron micrograph of myofibrils (Myf) of the pharyngeal muscle demonstrating the striated nature and collagenous matrix between muscle fibers. Scale bar = 1 µm. (e) The striated muscle (StM) contains multiple nuclei (N) as in typical vertebrate StM. H&E stain. Scale bar = 50 µm. (f) Transmission electron micrograph of StM fibers and nucleus (N). The striations are clear and demonstrate the typical banding pattern observed in vertebrates including the Z line (Z), M band (MB), A band (AB), I zone (IZ), and H zone (HZ). Scale bar = 200 nm. (g) Cross-sectional light micrograph of StM fibers illustrating the myomeres (Myo) separated by myosepta (Msp). H&E stain. Scale bar = 100 µm.

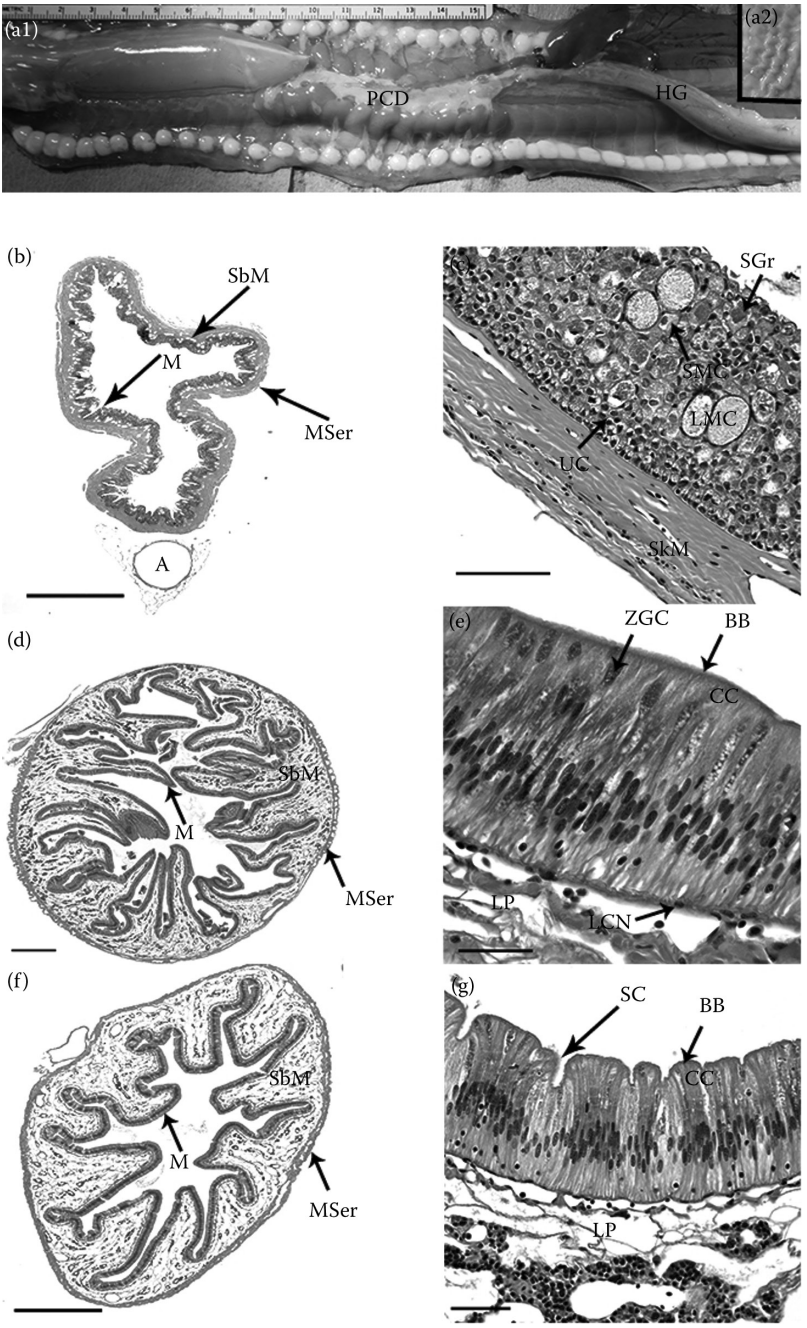

Figure 1.5 **(See color insert.)** (*Continued*)

heart where cross-striated muscle fibers cross the intestine (Adam, 1963; Andrew and Hickman, 1974). However, both foregut and hindgut are comprised of three layers: mucosa (M), submucosa (SbM), and *Muscularis serosa* (Figure 1.5b,d,f) (Adam, 1963; Andrew and Hickman, 1974). Although not previously acknowledged, there are indeed differences along the length of the hindgut, which will be discussed herein.

Foregut

The foregut contains a distinct cellular makeup, vastly different from the hindgut, but akin to the skin. Resting upon the basement membrane, are undifferentiated cells, which migrate upward to become either mature epithelial cells, small mucous cells, or large mucous cells (Figures 1.5c and 1.6a, b1, and b2). Uniquely, hagfish restrict all mucous cells to the foregut (Appy and Anderson, 1981; Menke et al., 2011). There are also secretory granulocytes (SGr) containing acidophilic granules, which are likely peptidases used to further enhance digestion (Figure 1.5c). The surface of this epithelium is covered with microridges (MRs) with no apparent pattern and as in the skin, function to reduce friction and aid in the progression of mucous and food down the tract (Figures 1.6a, b1, and b2). Irregularly shaped epithelial cells have clear borders

***Figure 1.5* (*Continued*)** Alimentary canal. (a1) Gross representation of the straight intestinal tube of the Pacific hagfish. Lacking a stomach, the hagfish intestine begins with the pharyngocutaneous duct (PCD), which runs alongside the gills. Posterior to the cardiac striations near the liver, the hindgut (HG) appears with distinct morphology. (a2) Mucosal surface of the hindgut. Large, permanent zigzag folds are used to enhance the surface area and may change color with nutritional status. (b) Cross-section of the PCD and corresponding intestinal artery (a). The intestine is composed of three layers: the outer *M. serosa* (MSer), a submucosa (SbM), and the mucosal layer (M). H&E stain. Scale bar = 1 mm. (c) Sagittal section of the PCD, displaying the SbM and the cellular components of the mucosa, which like the skin include, undifferentiated cells (UC), small mucous cells (SMC), large mucous cells (LMC), and secretory granules (SGr). H&E stain. Scale bar = 100 µm. (d) Cross-section of the anterior hindgut displaying the three layers: mucosa (M), submucosa (SbM), and *M. serosa* (MSer). H&E stain. Scale bar = 1 mm. (e) Sagittal plane of the anterior hindgut with a distinct morphology in comparison to the PCD. Atop a lamina propria (LP) rest the columnar cells (CC) with a brush border (BB). Interspersed among these cells are zymogen granule cells (ZGC) with acidic digestive enzymes. Also present are lymphatic cell nuclei (LCN) for immunity. H&E stain. Scale bar = 100 µm. (f) Transverse section of the posterior hindgut. Again the three layers are present [*M. serosa* (MSer), submucosa (SbM), and mucosa (M)], but with reduced infolding in comparison to the anterior hindgut. H&E stain. Scale bar = 1 mm. (g) Transverse section of the posterior hindgut. Resting upon an LP are the CCs with a BB, however also present are secretory cells (SC) of unknown function. H&E stain. Scale bar = 100 µm.

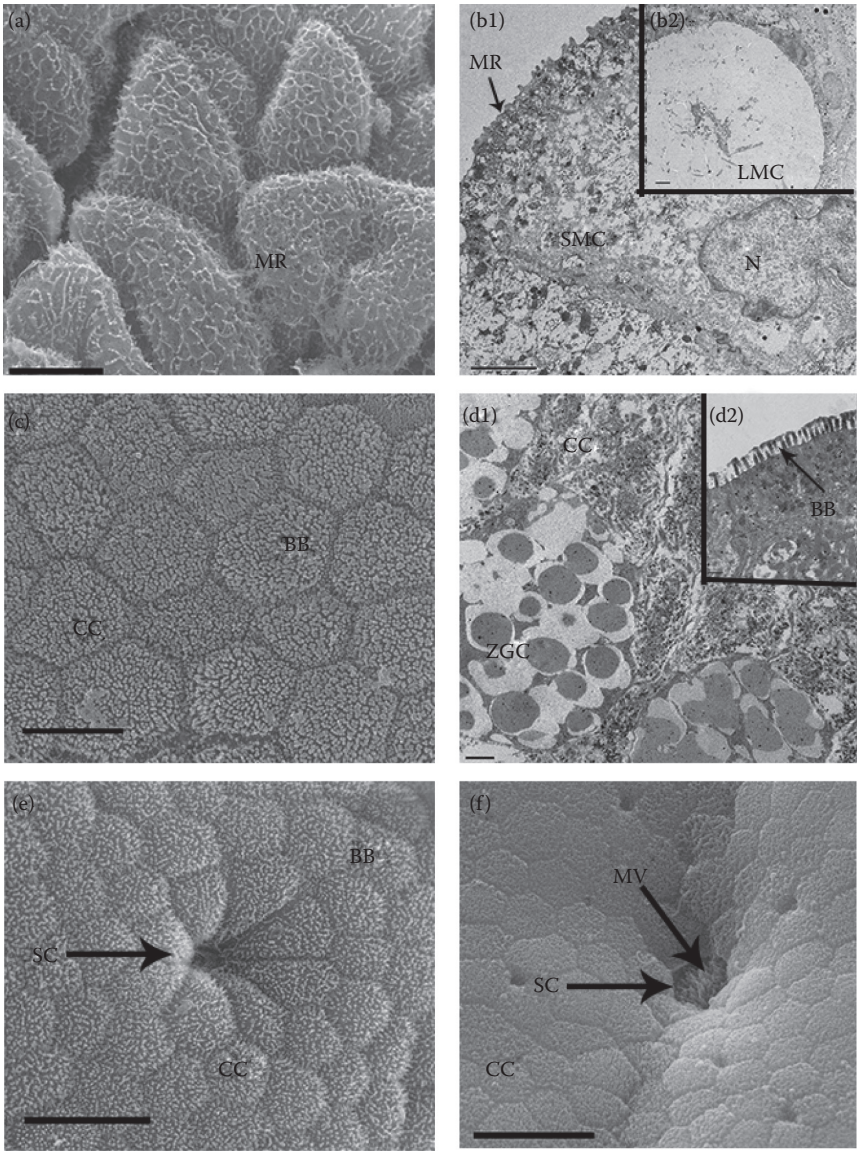

Figure 1.6 Alimentary canal. (a) Scanning electron micrograph of the pharyngocutaneous duct demonstrating the abundance of microridges (MR) on irregularly shaped epithelial cells. Scale bar = 5 µm. (b1) Transmission electron micrograph of the MRs atop a small mucous cell (SMC) with the typical basolaterally located nucleus (N). Scale bar = 2 µm. (b2) The disperse nature of the cytoplasm within the large mucous cells (LMC) of the PCD. Scale bar = 2 µm. (*Continued*)

with distinct cell–cell junctions and deeper furrows occur between cells, unlike the typical squamous cell covering of other vertebrate foreguts (Figure 1.6b1).

Beneath the basement membrane (BM) is a *lamina propria* (LP), an area rich in vasculature and adipose tissue. The submucosa (SbM) contains connective tissue (CT), lymph, and blood vessels, as well as varying amounts of adipose depending on the nutritional state (Adam, 1963; Andrew and Hickman, 1974) and dispersed lymph vessels that have sometimes been referred to as a diffuse spleen (Andrew and Hickman, 1974). The submucosa functions to provide turgidity to the intestinal walls, whereas the *M. serosa* aids in transport of nutrients by applying peristaltic pressures, with assistance required from body undulation (Andrew and Hickman, 1974). Not pictured here is the transition from foregut to hindgut, which lacks all specialized cells and contains only transitional epithelium.

Hindgut

The diameter of the hindgut measures 1–2 cm, becoming thinner toward the posterior end and changing color with nutritional status (Adam, 1963). It contains approximately 10 large, permanent zigzag folds which become somewhat diffuse in the preanal or anal regions (Figure 1.5a2). This is most likely due to the fact that absorption is reduced in these areas, as most of the nutrients have been absorbed and waste remains. The cells of the mucosal region are simple, columnar cells (CC) up to 250 μm in length (Figures 1.5e and g). They exhibit palpable polarization and a brush border (BB) to enhance surface area and aid in passage of food (Figures 1.6c, d1, d2, e, and f). Constituents that form peritrophic sacs are also secreted in this segment, which prevent bacterial penetration while allowing enzymatic penetration. These sacs enshroud the waste to be excreted (Adam, 1963; Hardisty, 1979). Interspersed among the columnar cells are zymogen granule cells (ZGCs) containing large, acidophilic secretory granules which have been likened to pancreatic enzymes and therefore, all digestion is thought to occur in the hindgut (Adam, 1963; Andrew and Hickman, 1974). They are easily identifiable

***Figure 1.6* (*Continued*)** (c) Scanning electron micrograph of the anterior hindgut displaying the extensive brush border (BB) atop the columnar cells (CC). Scale bar = 5 μm. (d1) Transmission electron microscopy of the zymogen granule cells (ZGC) among the CCs with a BB. Scale bar = 2 μm. (d2) Transmission electron microscopy detailing the fine BB lining the cells of the hindgut. Scale bar = 0.5 μm. (e) Scanning electron micrograph of a secretory cell (SC) surrounded by CCs covered with a BB. Scale bar = 10 μm. (f) Scanning electron micrograph of the various-sized pores within the CCs of the posterior hindgut. The central secretory cell (SC) appears to house microvilli (MV) of unknown function. The smaller pores are predicted to play a role in water regulation. Scale bar = 10 μm.

due to a single nucleolus in the nucleus along with a tapered apex, all of which is contained within a pit reminiscent of the mammalian pancreatic acinar cell (Adam, 1963; Appy and Anderson, 1981). Two distinct types of granules appear to reside within zymogen granule cell, a lightly stained, less-dense granule that is seemingly more basophilic than the alternative more-dense acidophilic granules (Figure 1.5e). These specialized epithelia rest upon a *lamina propria* (LP) containing dense connective tissue (CT) and numerous capillaries. At the interface between the basement membrane (BM) and lamina propria (LP) are distinct nuclei, which are thought to represent lymphatic cell nuclei (LCN), a probable necessity at an internal/external junction, given the feeding environment of the hagfish (Figure 1.5e). Similar to lamprey, the mucosal region of hagfish contains more absorptive cells than secretory cells (Appy and Anderson, 1981). However, the number of secretory cells (SC) appears to increase as you move down the intestine and become more diffuse toward the cloacal region (Figure 1.5g). These cells appear to group and form a secretory cleft or pit, distinct from the surrounding columnar epithelium (more lightly stained and a reduced BB), appearing pore-like in the SEM images (Figures 1.6e and f). The mucosal mucous lubricates the food and slows down diffusion of nutrients while preventing foreign invasion (Rogers, 1983; Clark and Summers, 2012). The submucosa and *M. serosa* function as mentioned above.

Liver

Located caudal to the portal heart, the liver (L) is contiguous with the gall bladder (GB) via a bile duct (BD) off the smaller, rostral lobe (Figure 1.7a) (Adam, 1963). The hagfish liver is a large, two-lobed tubular organ that comprises ~3.5% of the total body weight and is surrounded by a thin layer of squamous epithelia (Anderson and Haslewood, 1967; Mugnaini and Harboe, 1967; Yousen, 1979; Umezu et al., 2012). It is structurally similar to a mammalian liver, suggesting that it was acquired early on in vertebrate phylogeny (Umezu et al., 2012). Hagfish hepatocytes (HE) have polarity, which is obvious due to apical microvilli (MV) (Mugnaini and Harboe, 1967). Also notable are the lipid deposits (LI) in the liver, giving hepatocytes a vacuolated appearance (Figures 1.7b and c). This fatty status corresponds well with the elasmobranch liver, which is utilized in flotation and intermediary metabolism (Inui and Gorbman, 1978).

The hepatocytes are exocrine, producing bile and passing it through multiple canaliculi (Ci), which merge to form the bile duct (BD), leading to the gall bladder (GB) for storage (Figure 1.7c). A close-up of the caniliculus (Figure 1.7d) shows a highly interdigitated surface epithelium with numerous microvilli (MV), with secretory products (SPs) in the lumen (L). A separate bile duct lined with a columnar epithelium (CE) and surrounded by

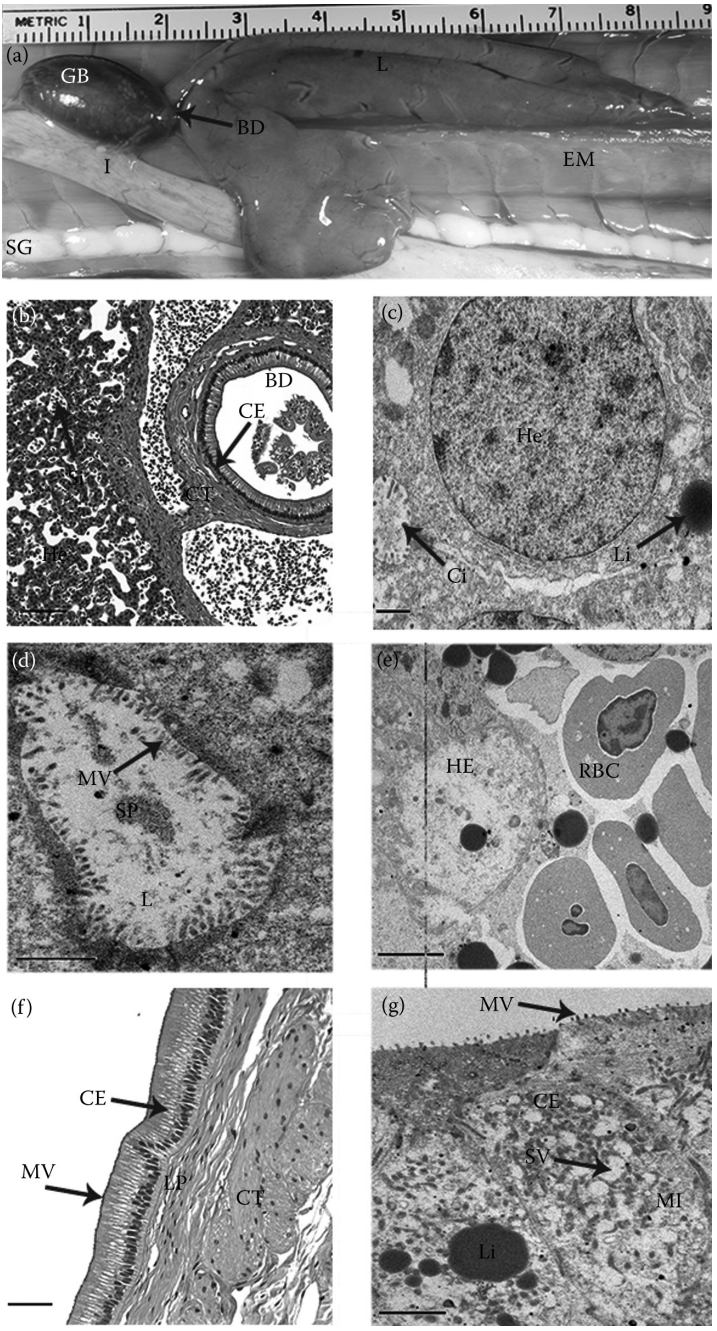

Figure 1.7 (**See color insert.**) (*Continued*)

connective tissue permits passage into the intestine (Figure 1.7b) (Adam, 1963; Umezu et al., 2012). Whether any connection exists between bile ducts or whether the portal triad exists is unknown to date (Umezu et al., 2012). The bile itself contains a bile alcohol, myxinol disulfate, which is less effective than vertebrate bile alcohols (Anderson and Haslewood, 1967).

Hepatocytes are also responsible for the regulation of blood glucose and proteins, with insulin being released from the liver. However, hepatectomized hagfish live 5–30 days, with no lowering of blood glucose, suggesting additional regulation and quite possibly intestinal supplementation (Fänge et al., 1963; Inui and Gorbman, 1978; Malte and Lomholt, 1998). Only one enzyme of the ornithine-urea cycle (arginase) has been detected in hagfish liver tissue (Read, 1975). While urea is seemingly unable to be produced, the liver is speculated to be excretory due to transport of organic acids from the blood into the bile, a task that the primitive archinephric duct is incapable of. Blood stems from the *vena supra-intestinalis* and right jugular vein into three types of vessels: bile-ductule-associated, nonassociated (such as portal veins lined with epithelium), and sinusoids (Si) draining to the central vein (Figure 1.7b) (Fänge et al., 1963). Red blood cells (RBC) are notable within these vessels where exchange of material occurs over a thin endothelium and peritubular connective tissue with foot processes for an increased surface area (Figure 1.7e) (Malte and Lomholt, 1998).

Gall bladder

The gall bladder is responsible for the storage of bile received from the liver via hepatic ducts, until release is prompted by cholinergic signals

***Figure 1.7* (*Continued*)** Liver and gall bladder. (a) Gross morphological details of the bi-lobed liver (L) and gall bladder (GB), attached via a bile duct (BD). Ducts also lead to the intestine (I) for bile distribution. EM, epaxial muscle; SG, slime gland. (b) Light micrograph of the hepatocytes (He) and sinusoids (Si) within, alongside a BD lined with columnar epithelium (CE) and supported by connective tissue (CT). H&E stain. Scale bar = 100 µm. (c) Transmission electron micrograph of an HE. Spherically shaped they are surrounded by lipid deposits (LI) and canaliculi (Ci) for transport. Scale bar = 1 µm. (d) A single, microvilliated (MV) canaliculus within a hagfish liver. The lumen (L) contains multiple secretory products (SP). Scale bar = 1 µm. (e) Transmission electron micrograph displaying the exchange capacity within the liver as the hepatocytes (HE) are surrounded by capillaries filled with erythrocytes (RBC). Scale bar = 5 µm. (f) GB wall. A simple CE topped with MV resting on an lamina propria (LP) and CT layer. Beneath this is the muscular layer necessary to contract the GB and expel bile. H&E stain. Scale bar = 100 µm. (g) Epithelial surface of the GB. The CE houses MV. Within the cells themselves, organelles are not present near the surface but include mitochondria (MI), lipid droplets (LI), and numerous vacuoles and vesicles (SV). Scale bar = 2 µm.

(Fänge et al., 1963; Anderson and Haslewood, 1967; Malte and Lomholt, 1998). Located caudal to the portal heart, it is obvious due to its bluish-green coloration (Figure 1.7a). The inside wall is lined with the tall, simple columnar epithelium resting on a basement membrane, which in combination with the underlying lamina propria composes the mucosal layer. Beneath the mucosa is the submucosa consisting of connective tissue and blood vessels, all of which are surrounded by a well-developed smooth muscle used for the propulsion of bile (Inui and Gorbman, 1978; Morrison et al., 2006). The perimuscular layer is again connective tissue and the surrounding serosal layer is continuous with the peritoneum and physically attaches the gall bladder to the liver and epaxial muscle.

Ultrastructurally, the apical surface of the columnar cells contains a brush border of ~0.175 μm long microvilli appearing consistently (Figures 1.7f and g). Apart from obviously increasing the surface area, the microvilli do not have a defined functional significance. The function of the gall bladder is primarily a storage of bile salts for fat emulsification and also enzyme maturation. The functional significance of hagfish gall bladder is as yet undefined, however with lipid granules (LI) and numerous mitochondria (MI) present, it suggests that the highly microvilliated surface has an absorptive or secretory capacity. The content of these microvilli does not appear to differ from that of the cytoplasm in the rest of the cell. Typically, the cytoplasm is of consistent electron density and the first ~2.5–3.0 μm of the apical region of the cell is devoid of organelles. Below this area is filled with multiple vacuoles and vesicles (SV). Studies conducted in some vertebrates suggest that some vesicles form by pinocytosis for the consumption of water and lipids (LI), whereas other vesicles are contingents of the endoplasmic reticulum used for trafficking to the Golgi apparatus in the supranuclear zone (Johnson et al., 1962; Inui and Gorbman, 1978).

Numerous elongated mitochondria (MI) observed with higher concentrations typically in the infranuclear region, associating with the endoplasmic reticulum. Various-sized lipid deposits (LI) were observed, although not membrane-bound (Figure 1.7g).

Renal system

Hagfish have two retroperitoneal archinephric ducts (AD) placed laterally on either side of the dorsal aorta (DA) and postcardinal vein (Figure 1.8a). Perfusion with Coomassie Brilliant Blue helped highlight distinct very large, independent glomeruli (G) joined by ductile tubule location as distinct circular structures along the archinephric duct (Figure 1.8b). Arising blindly just anteriorly to the liver, these ducts store urine before output into the cloaca via posterior ureters. The urine output is low at 4–10 mL/kg/day and is believed to be related to glomerular filtration rate (Andrew and Hickman, 1974; Hardisty, 1979; Fels et al., 1998; Riegel and Bardack, 1998). The 30–40

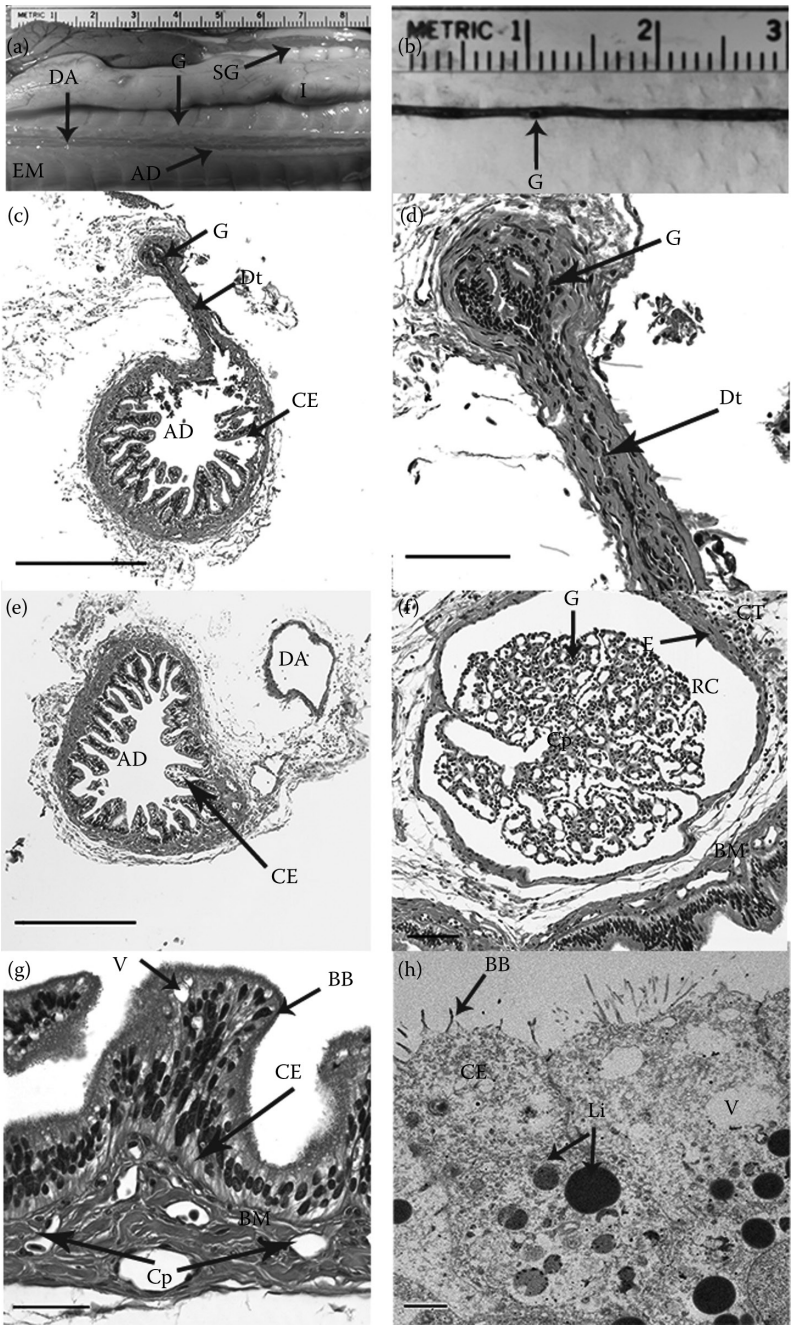

Figure 1.8 (**See color insert.**) (*Continued*)

ovoid renal corpuscles (RC) are each individually connected to the archinephric duct via ductile tubules (Dt). The renal corpuscles house the glomeruli (G) and dissipate toward the caudal end (Figures 1.8b, c, d, and f).

The archinephric duct is lined with simple columnar or cuboidal epithelia (CE), resting on a basement membrane (Figure 1.8e) (Yousen, 1979; Fels et al., 1998). There is an obvious brush border of long, straight microvilli (MV) and along with vacuoles (V) aids in the absorption of materials during the extended time when urine is stored (Andrew and Hickman, 1974; Yousen, 1979; Fels et al., 1998). Besides large vacuoles, vesicles, inclusion bodies, and apical pits are observed among a tubular network on the apical surface. Surrounding the duct is a connective tissue network.

The blood supply is entirely arterial, with arteries stemming from the dorsal aorta and thinning into an extensive capillary network (CP) within the glomerulus (Figures 1.8f and g). There are generally three efferent arterioles through which blood can exit the system into the postcardinal vein. The corpuscle itself is lined with mesangial cells, apart from the thinnest capillary, which contains endothelial cells (E) alone (Figure 1.8f). Within the columnar cells are multiple lipid droplets (LI) of varying size and staining intensity (Figure 1.8h). It is possible that these represent different functional components, but this is yet to be elucidated.

Glomeruli function to produce peritoneal fluid using a central mass of cells as a phagocytic filter for the blood and peritoneal fluid (Fänge, 1963; Riegel and Bardack, 1998). Although potassium, magnesium, and sulfate are excreted in the glomerular filtrate, it seems that sodium is able to be resorbed (McInerney, 1974). The renal system is responsible for the maintenance of the ionic and osmotic composition through the secretion

---

***Figure 1.8* (*Continued*)** Archinephric duct (AD). (a) Hagfish have two ADs; one on either side of the dorsal aorta (DA). Large, visible glomeruli (G) are seen along the length of the duct. I, intestine; EM, epaxial muscle; SG, slime gland. (b) Excised AD stained with Coomassie Blue to increase glomeruli (G) visibility. (c) Cross-section of the AD and associated glomerulus (G). The duct is lined with a columnar epithelium (CE) and connects to the glomerulus via a small ductule (Dt). H&E stain. Scale bar = 500 µm. (d) Detailed images of the glomerulus (G), connected to the Dt. H&E stain. Scale bar = 100 µm. (e) Cross-section of the CE lined AD and associated DA. H&E stain. Scale bar = 500 µm. (f) Sagittal section of a glomerulus (G) inside the surrounding connective tissue (CT). The glomerulus is housed within a renal corpuscle (RC) lined with an endothelial layer (E) and filled with numerous capillaries (Cp). BM, basement membrane. H&E stain. Scale bar = 100 µm. (g) Sagittal section of the AD highlighting the numerous vacuoles (V) within the CE that are topped with a brush border (BB). The transport capacity is highlighted beneath the BM where multiple capillaries (Cp) are observed. H&E stain. Scale bar = 50 µm. (h) Transmission electron micrograph of the long, thin BB atop cells filled with multiple vacuoles (V) and lipid droplets (LI). Scale bar = 5 µm.